Design Considerations of a Low-Noise Receiver Front-End and its Spiral Coil for Portable NMR Screening

Diyang Zhao, Ka-Meng Lei, Pui-In Mak, Man-Kay Law and Rui P. Martins [1]

The State Key Laboratory of Analog and Mixed-Signal VLSI and FST ECE, University of Macau, Macao, China
1 – On leave from Instituto Superior Técnico, Universidade de Lisboa, Portugal (E-mail: pimak@umac.mo)

***Abstract*—This paper reports the co-design of a low-noise receiver front-end and its exciting-sensing coil for portable nuclear magnetic resonance (NMR) screening of chemical/biological droplets operating at 21.3MHz (0.5T magnet). To minimize the noise contribution of the receiver front-end and its coil compared to the induced signal, EM analysis is involved to optimize the geometry of the off-chip coil with the input-referred noise of the receiver front-end taken into account. By choosing a proper geometry of the coil, the resulted SNR of the receiver front-end was shown to be maximized with the dedicated input-referred noise of the receiver. Simulated in 180nm CMOS, the receiver front-end shows an input-referred noise as low as 920.11pV/$\sqrt{\text{Hz}}$ at 25.2mW of power, and the estimated die area is ~2mm^2.**

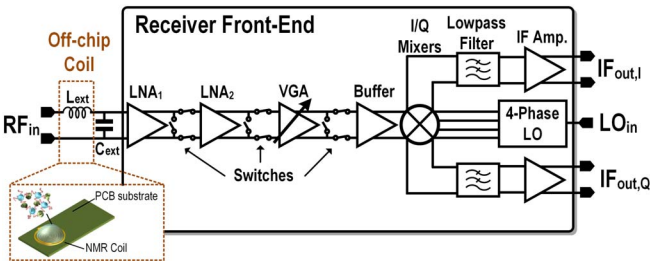

Fig. 1 Proposed low-noise receiver front-end with its exciting-sensing coil for NMR operation on a chemical/biological sample.

I. Introduction

Nuclear magnetic resonance (NMR) represents a physical phenomenon in which nuclei absorb and re-emit radio-frequency (RF) magnetic waves, in the presence of a strong and static magnetic field (from a permanent or superconducting magnet), which allows the observation of specific quantum mechanical magnetic properties of the atomic nucleus. As the environment of the nuclei influences the detailed resonance behavior, NMR-based methods are amongst the most powerful analysis tools in modern chemistry, biological assay and pharmacology. Since, in principle, scaling down the size of the exciting-sensing coil increases the spin sensitivity of the NMR receiver [1], it will be promising to build a compact NMR system for chemical/biological micro-reactors using integrated circuits to achieve higher sensitivity and portability, as well as low cost.

The continuous progress of microelectronics offers low-cost to novel applications of NMR with high specificity for the detection and quantification of biological samples. Notably, research efforts have been focused in NMR miniaturization. The 130nm CMOS transceiver in [2] includes a low-noise amplifier (LNA), I/Q mixers, lowpass filters and variable-gain amplifiers (VGA) for the receiver I and Q paths. The operating frequency covers 5 to 300MHz suitable for a variety of chemical samples testing. In [3], the 180nm CMOS NMR transceiver includes a LNA, VGA and mixers, with an operating frequency of ~21MHz to detect the biological objects. Both works are highly-integrated solutions, yet did not consider the noise generated by the coil. In [4], the 300MHz 130nm CMOS receiver integrated an on-chip coil, tuning capacitors, a LNA, I/Q mixers and IF amplifiers. They introduced the coil optimization together with the input-referred noise of the receiver. Yet, it only involved the noise generated by the coil and receiver, but not yet determining the signal coupling capability of the coil. Since the overall SNR of the signal is crucial to the analysis, the signal intensity itself should also be considered.

In this paper, a systematic approach to design and optimize a 21.3MHz (0.5T) low-noise receiver front-end for portable NMR systems is presented. It includes a two-stage LNA to minimize the noise of subsequent circuitry, and I/Q mixers to downconvert the signal to intermediate frequency (IF) for lowpass filtering. The geometry of the coil is optimized via Electromagnetic (EM) simulations with the consideration of signal inducing capability, as well as the coil's and receiver's thermal noises.

II. Proposed Low-Noise NMR Receiver Front-End

The block diagram of the receiver front-end with an off-chip NMR coil is depicted in Fig. 1. The forefront two-stage LNA (LNA_1 and LNA_2) is followed by a VGA and buffers before driving the I/Q mixers for downconversion. The four-phase IF outputs (I/Q and differential) are lowpass filtered to eliminate the high frequency noise and an IF amplifier further boosts the signal level. To prevent unwanted coupling of the excitation signal to the output signals, dedicated switches are added to disconnect the stages and turn each RF stage into isolated blocks in the excitation phase. The key concerns of the building blocks are introduced next.

A. LNA_1 and LNA_2

For concurrent low noise and low power, the design of the LNA_1 [Fig. 2(a)] is crucial. This work uses a complementary common-source structure for current reuse similar to [5]. The differential topology minimizes the common-mode coupling. A common-mode feedback (CMFB) circuit stabilizes the output

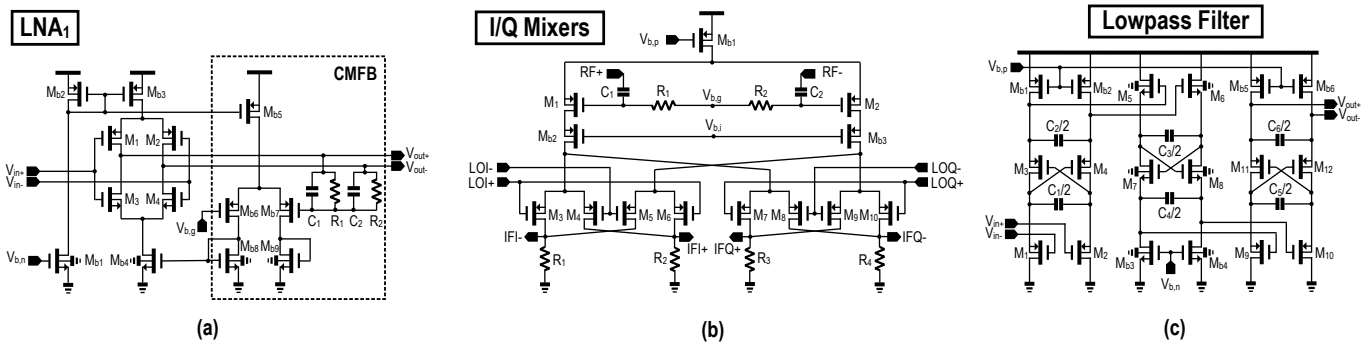

Fig. 2 Schematics of the (a) complementary common-source LNA_1 with an output CMFB (LNA_2 is similar). (b) double-balanced active I/Q mixers. (c) 6th-order source-follower-based lowpass filter.

DC level. Compensation capacitors (C_1 and C_2) are parallelized to the CM-level sensing resistors (R_1 and R_2) to stabilize the CMFB loop. In addition, to eliminate the substrate noise coupling from digital circuitry of the clock signal, a deep n-well is adopted to isolate the NMOS input pair from the p-type substrate.

To reduce the noise from the mixer and subsequent stages, the LNA_2 is introduced. The offset from LNA_1 may become large at the input of the 2nd stage since the gain of LNA_1 is set at ~30 V/V. This offset may potentially saturate the subsequent stages. To solve this, LNA_1 and LNA_2 should be AC-coupled via a RC-highpass network. The circuit topology of LNA_2 is similar to LNA_1, but with a smaller bias current due to a relaxed noise requirement.

B. VGA

The amplitude of the received signal depends on the volume and composition of the sample under NMR. Thus, to ensure that the receiver is capable of detecting different kinds of samples, a VGA (not shown) is essential to optimize the signal level. It is built by a common-source amplifier with a tunable voltage-controlled resistor at the drains of the differential pair.

C. I/Q Mixers

After amplification, the RF signal is downconverted to the IF by a pair of double-balanced I/Q mixers [Fig. 2(b)], which reduce the noise figure (double sideband) and LO-to-IF feedthrough. The low IF value reduces the disturbance of the flicker noise. The mixer is constructed by PMOS transistors to reduce the flicker noise and substrate coupling from/to another part of the system. To avoid LO-to-RF leakage, a pair of buffers (source followers) is introduced at the input of the mixers.

D. Lowpass Filter

The lowpass filter suppresses the out-of-band noise and the unwanted high-frequency signal generated by the I/Q mixers. While the cut-off frequency is typically set at several kHz for the NMR applications, conventional RC-based lowpass filters will demand huge area to realize the time constant. Here, the source-follower-based lowpass filter [Fig. 2(c)] [6] is selected. It can provide a very low cut-off frequency by reducing the transconductance of the transistors, thereby also saving power. By using the transistorized positive feedback, such filter can synthesize complex poles in a single branch reducing the circuit complexity and unwanted parasitic poles. To implement a 6th-order Butterworth lowpass filter, three Biquads are cascaded. The cut-off frequency can be easily tuned by the bias current.

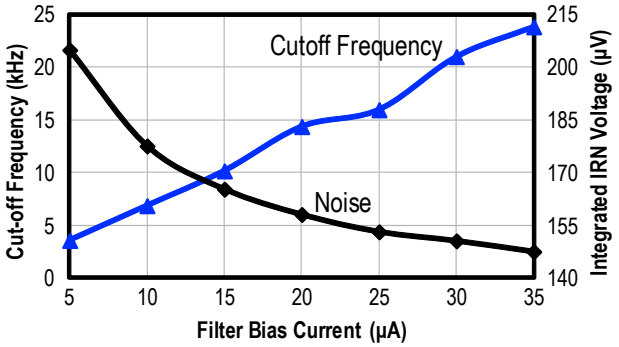

Fig. 3 Filter cutoff frequency and integrated noise against bias current.

TABLE I.
COMPARISON WITH OTHER NMR SYSTEM RECEIVERS.

	[2]	[3]	[4]	This work (Simulation)
Technology (nm)	130	180	130	180
Frequency (MHz)	5-300	20	300	21.3
Voltage Supply (V)	1.5	3.3	1.8	1.8
Current (mA)	12	25	50	14
IRN (nV/$\sqrt{\text{Hz}}$)	3.5	1.26	×	0.92
Gain-Control	✓	×	×	✓
On-Chip Filter	✓	×	×	✓

III. RECEIVER FRONT-END SIMULATION RESULTS

From post-layout simulations, the VGA offers a gain range of ~17 to 26.3dB with the –3dB bandwidth reduced from 310 to 110 MHz, which is large enough for the targeted RF signal at 21.3MHz. In overall, the gain of the RF part can be tuned from 62.7 to 78.9dB, with the bandwidth within 39.4 to 51.8MHz.

The 6th-order lowpass filter is simulated with a nominal bias current of 20μA. The cutoff frequency is set at 15kHz, and is tunable from 3.56 to 23.8kHz by adjusting the bias current. The cutoff frequency versus the bias current is plotted in Fig. 3 together with the integrated input-referred noise of the filter. It can be seen that with a lower bias current, the noise goes up as

expected due to the lower transconductance. Yet, this fact has negligible effect to the receiver as the noise is dominated by the forefront LNA.

After layout, the estimated chip area is ~2mm^2. The receiver totally draws 14mA from a 1.8V supply. The input-referred noise is minimized to 920.11pV/$\sqrt{\text{Hz}}$ and the SNR is still 18dB at 1μV input. Table I compares this work with [2]-[4].

IV. Coil Optimization

A. Signal and Noise Analysis of Coil and Receiver

As shown in Fig. 1, there is an off-chip coil necessary for the receiver to perform NMR. It is possible to obtain the inductance of the coil as,

$$L_{ext} = K_1 \mu \frac{N^2 d_{avg}}{1+K_2 \rho} \quad (1)$$

where N is the turns of the coil, μ is magnetic constant, K_1, K_2 are layout dependent coefficients, ρ represent how hollow the inductor is and d_{avg} is the average diameter of the coil [7]. To let the off-chip coil and capacitor reach the desire oscillation frequency f_{osc} while offering a passive pre-gain, the desired value of the off-chip capacitor can be calculated from,

$$C_{ext} = \frac{1}{4\pi^2 {f_{osc}}^2 L_{ext}} \quad (2)$$

Thus, the quality factor of the off-chip inductor can be found as,

$$Q = \frac{\omega L_{ext}}{R_{coil}} = \frac{2\pi f_{osc} L_{ext}}{R_{coil}} \quad (3)$$

The coil has an internal resistance R_{coil} which depends on the geometry of the coils and the conductivity of the fabricated materials. The resistance could be divided into three parts: ohmic, skin effect and proximity effect [8]. Such resistances not only degrade the passive pre-gain ($\sqrt{Q^2+1}$) of the LC tank, but also impose thermal noise on the receiver.

The thermal noise of the resistor in the receiver coil is described by the Nyquist formula,

$$\overline{V^2_{noise,coil}} = 4k_B T R_{coil} \quad (4)$$

where k_B is Boltzmann's constant and T is the resistor's absolute temperature.

The induced voltage V_{EMF} of the coil can be expressed as,

$$V_{\text{EMF}} = -\int \left(\frac{\partial}{\partial t}\right)(B_{xy} M_0)\, dV_s \quad (5)$$

where M_0 is the nuclear magnetization which is proportional to the field strength B_0, B_{xy} is the field produced by the unit current passing through the coil at M_0 and V_{s} is the sample volume of interest [9]. To compare the magnitude of V_{EMF} for different coil structures over same samples volumes, the average B_{xy} produced by the coils can be simulated in EM simulation tools and V_{EMF} should be proportional to B_{xy}, given that the magnetization of the nuclei are the same for both cases.

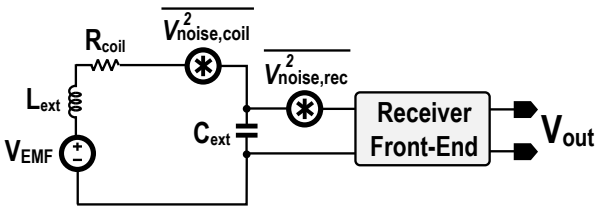

Fig. 4 Noise equivalent circuit of the receiver front-end with the coil.

The turns of the coil can be changed in different situations to befit the receiver. If the number of turn is increased, V_{EMF} should also be increased. However, inductance and resistance will rise jointly due to the geometry change. Thus, V_{EMF} and thermal noise of the coil are affected. It is hard to analytically optimize the turns of the coil for the best SNR. To this point, computational optimization of the coil becomes more feasible.

To optimize the coil, the system of Fig. 4 was simulated with Cadence to get the SNR of the receiver front-end. The signal at the output of the receiver is the induced voltage amplified by the LC tank and the receiver gain A_{rec}, thus the signal is given as,

$$Signal = V_{\text{EMF}} \cdot \sqrt{Q^2+1} \cdot A_{rec} \quad (6)$$

The noise of the system is composed by two parts: thermal noise of the coil that is amplified by the LC tank and the noise of the receiver, which appears at the output of the receiver together as,

$$Noise = \sqrt{\overline{V^2_{noise,coil}}(Q^2+1) + \overline{V^2_{noise,rec}}} \cdot A_{rec} \quad (7)$$

Taking the thermal noise of the coil resistance and the noise of the RF stages into account, the SNR of the coil with receiver front-end as a whole can be determined with,

$$SNR = \frac{Signal}{Noise} = \frac{V_{\text{EMF}}\sqrt{Q^2+1}}{\sqrt{\overline{V^2_{noise,coil}}(Q^2+1)+\overline{V^2_{noise,rec}}}} \quad (8)$$

From (8), it can be found that the turn number of the coil will concurrently affect the magnitude of signal and noise since both V_{EMF}, Q and $\overline{V^2_{noise,coil}}$ is dependent on coil geometry. To further optimize the coil, a systematic study involving the EM analysis tool and circuit simulations are presented next.

B. Coil Parameter Simulations with COMSOL

When a receiver is being employed for NMR purposes, there is a coil placing at the front of the PCB board and the droplet sample is at the center of the coil (for the case of planar coil) to generate the RF signal. The coil with sample on the PCB board is sketched in Fig. 1. To obtain the relationship between the turns of the coil and induced voltage to the coil, COMSOL is employed to simulate the coil parameters and the magnetic parameters for calculation. It accounts the coil inductance and resistance, and the average of the induced magnetic field on the water droplet. The width of the conductors and space between them is set to 0.15mm. The

TABLE II.
COMPARISON BETWEEN THE COMSOL RESULT AND THE REAL COIL MEASUREMENT @ 21.3 MHZ. ($\sigma_{Cu} = 5.96 \times 10^7 S/m$)

	COMSOL Simulation			Coil Measurement		
Turns	L(nH)	R(Ω)	Q	L(nH)	R(Ω)	Q
7	143.20	0.68	28.29	146.17	0.67	28.78
9	264.86	1.05	33.66	266.10	1.05	33.43
12	546.70	1.76	41.51	545.60	1.75	41.13
15	966.98	2.64	49.05	1009.53	2.80	47.57

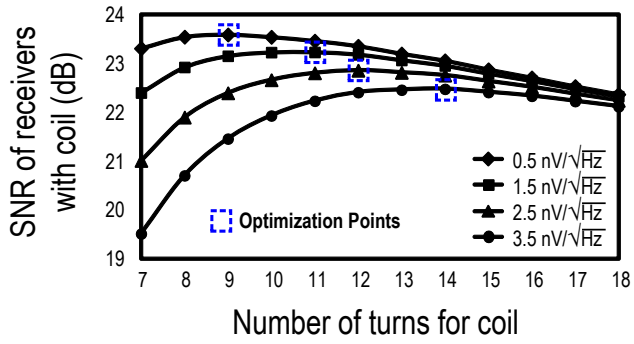

Fig. 5 SNR under different noise performances of the receiver versus the turns of the coils.

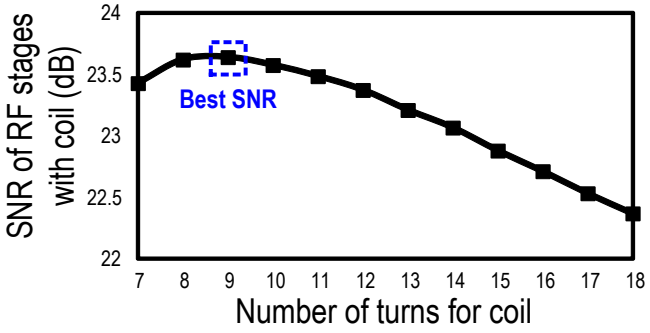

Fig. 6 SNR of the RF stages for the receiver versus the turns of the coils simulated in Cadence.

height of the conductors is set to 19μm. Normally, the coil size cannot be too large or too small, thus we limited the turns of the coil within 7 to 18. If increasing the turns, the coil inductance and resistance will raise together, so as the generated magnetic field. To assess the results, we measured the coil inductance and resistance with turns 7, 9, 12 and 15 and compared with the results in COMSOL (Table II). Those results are highly consistent with the real coil measurements.

From (8), the noise generated in the receiver will affect the overall SNR. Yet, the noise of the receiver front-end is not the same, thus the best solution for the turns of the coil may change with respect to the noise performance of the receiver. The mathematical SNR model from (8) of different input-referred noise level NMR systems were simulated with coil changing with their turns, as shown in Fig. 5. Here, the input-referred noise of the receiver ranged from 0.5 to 3.5nV/$\sqrt{\text{Hz}}$. When the input-referred noise goes up, the optimal turn of the coil rises as well. For the receiver that the input-referred noises are 0.5, 1.5, 2.5 and 3.5nV/$\sqrt{\text{Hz}}$, the turns of coil that offer the best performance are 9, 11, 12 and 14, respectively.

C. Coil Optimization for the NMR Receiver

For the designed receiver with the coil, the SNR versus the turns of the coil was simulated (post-layout simulation) in Cadence and plotted in Fig. 6. When the turns of the coil rise from 7 to 18 the calculated SNR peaks to 23.65 dB when the turn of the coil is 9, value selected for our receiver.

V. CONCLUSIONS

We reported the co-design of a low-noise receiver front-end and its exciting-sensing coil for portable NMR screening of chemical/biological droplets. To optimize the noise generated by the receiver and its coil, EM analysis is entailed to determine the geometry of the off-chip coil together with the input-referred noise of the receiver. It is shown that by choosing a proper geometry of the coil, the SNR of the receiver could be maximized with the dedicated input-referred noise of the receiver. Simulated in 180nm CMOS, the receiver front-end achieves an input-referred noise of 920.11 pV/$\sqrt{\text{Hz}}$. The power consumption is 25.2mW and the estimated chip area is ~2mm^2.

ACKNOWLEDGEMENTS

This work is partially funded by the University of Macau Honours College and Research Committee, as well as the Macao Science and Technology Development Fund - FDCT (033/ 2011/A2) and SKL funds.

REFERENCES

[1] R. Subramanian, M. M. Lam, and A. G. Webb, "RF microcoil design for practical NMR of mass-limited samples," *Journal of Magnetic Resonance*, vol. 133, pp. 227–231, Jul. 1998.

[2] J. Kim, B. Hammer, and R. Harjani, "A 5-300 MHz CMOS transceiver for multi-nuclear NMR spectroscopy," in *IEEE Custom Integrated Circuits Conference (CICC)*, San Jose, CA, Sep. 2012, pp. 1–4.

[3] N. Sun, T.-J. Yoon, H. Lee, W. Andress, R. Weissleder, and D. Han, "Palm NMR and 1-chip NMR," *IEEE Journal of Solid-State Circuits*, vol. 46, no.1, pp. 342–352, Jan. 2011.

[4] J. Anders, P. SanGiorgio, and G. Boero, "A fully integrated IQ-receiver for NMR microscopy," *Journal of Magnetic Resonance*, vol. 209, pp. 1–7, Dec. 2011.

[5] J. Anders and G. Boero, "A low-noise CMOS receiver frontend for MRI," in *IEEE Biomedical Circuits and Systems Conference*, Baltimore, MD, pp. 165–168, Nov. 2008.

[6] S. D'Amico, M. Conta and A. Baschirotto, "A 4.1-mW 10-MHz fourth-order source-follower-based continuous-time filter with 79-dB DR," *IEEE Journal of Solid-State Circuits*, vol. 41, no.12, pp. 2713–2719, Dec. 2006.

[7] S. S. Mohan, M. Hershenson, S. P. Boyd and T. H. Lee, "Simple accurate expressions for planar spiral inductancs," *IEEE Journal of Solid-State Circuits*, vol. 34, no. 10, pp. 1419–1424, Oct. 1999.

[8] T. L. Peck, R. L. Magin, and P. C. Lauterbur, "Design and analysis of microcoils for NMR microscopy," *Journal of Magnetic Resonance*, vol. 108, pp. 114–124, Feb. 1995.

[9] D. I. Hoult and R. E. Richards, "The signal-to-noise ratio of the nuclear magnetic resonance experiment," *Journal of Magnetic Resonance*, vol. 24, pp. 71–85, Mar. 1976.